

# Time-reversal symmetry breaking and the statistical properties of quantum systems

Georg Lenz† and Karol Życzkowski‡

† Fachbereich Physik, Universität-GHS Essen, 4300 Essen, Federal Republic of Germany

‡ Instytut Fizyki, Uniwersytet Jagielloński, ul. Reymonta 4, 30-059 Kraków, Poland

Received 30 March 1992, in final form 1 July 1992

**Abstract.** The breaking of the generalized time-reversal symmetry of a quantum chaotic system corresponds to a transition from orthogonal to unitary ensembles of random matrices. Investigating this transition for the circular ensembles of Dyson (applicable for time-dependent, periodic systems) we demonstrate and explain that there exists a relevant difference of the transition rate in comparison with the Gaussian ensembles appropriate for quantum conservative systems. The above supposition is supported by a numerical study of the eigenvalues and eigenvectors of the periodically kicked top.

## 1. Introduction

The statistical properties of quantized chaotic systems are known to be well described by ensembles of random matrices [1, 2]. Depending on the symmetry of the system one of the three universal ensembles are appropriate: the orthogonal ensemble (OE) describes systems with an anti-unitary symmetry (generalized time-reversal symmetry) while the unitary ensemble (UE) characterizes systems without such symmetry [3]. The third class, the symplectic ensemble (SE), corresponds to systems where the Kramers degeneracy occurs (half-integer spin and exactly one anti-unitary symmetry) [4].

Three Gaussian ensembles studied by Mehta [1] (GOE, GUE and GSE) are applicable for those conservative quantum systems, the classical counterparts of which exhibit global chaos. Related are the circular ensembles introduced later by Dyson [1] (COE, CUE and CSE) which allow one to describe the statistical properties of the classically chaotic, time-dependent, periodic systems. Interestingly the theory of random matrices predicts the same statistics of eigenvalues and eigenvectors for the corresponding Gaussian and circular ensembles [1].

The level spacing distribution  $P(S)$ , often used to characterize spectral fluctuations, is well approximated by the Wigner surmise

$$P(S) = \frac{\pi}{2} S \exp\left[-\frac{\pi S^2}{4}\right] \quad (1)$$

$$P(S) = \frac{32}{\pi^2} S^2 \exp\left[-\frac{4S^2}{\pi}\right] \quad (2)$$

$$P(S) = \left(\frac{64}{9\pi}\right)^3 S^4 \exp\left[-\frac{64S^2}{9\pi}\right] \quad (3)$$

for the orthogonal, unitary and symplectic ensemble, respectively [3]. It is worth noting that other measures of the statistical properties of the spectrum, like the two-point correlation function  $R_2(S)$ , the number variance  $\Sigma^2(L)$  or the spectral rigidity  $\Delta_3(L)$ , also have the identical form for both families of the Gaussian and circular ensembles (in the limit of large matrix size  $N$ ). Also the eigenvector statistics, the distribution of the squared moduli of components  $P(y)$ , is given for both kinds of ensembles (in the limit of  $N \rightarrow \infty$ ) by the same chi-square distribution [5, 6]

$$P(y) = \frac{(\beta/2)^{\beta/2}}{\Gamma(\beta/2)\langle y \rangle} \left( \frac{y}{\langle y \rangle} \right)^{\beta/2-1} \exp \left[ -\frac{\beta y}{2\langle y \rangle} \right] \quad (4)$$

where the number of degrees of freedom  $\beta$  is equal to 1, 2 and 4 for OE, UE and SE, respectively, and  $\langle y \rangle$  denotes the mean value of the eigenvector component. The above results of the theory of random matrices describe with an amazingly high accuracy the statistical properties of various dynamical systems [2, 6]. As a fourth universality class one can consider the diagonal matrices of real random elements in the case of Gaussian ensembles (or the unitary matrices with random eigenphases in the case of circular ensembles). Both ensembles display Poisson statistics in their spectra and are appropriate to describe classically regular systems [7].

Apart from systems pertaining to the different universality classes, one may consider a one-parameter family of systems which undergoes a continuous transition between two ensembles. Of great interest is the transition between the orthogonal and the unitary ensembles, since it corresponds to the breaking of a generalized anti-unitary symmetry in a dynamical system. The influence of (partial) time-reversal symmetry breaking for the statistical properties of the spectrum was first observed in [8]. Similar results were obtained by analyses of the conductance fluctuations of mesoscopic systems in an external magnetic field [9, 10]. In addition the OE–UE transition has been studied for model dynamical systems like billiards in a magnetic field [11], Aharonov–Bohm billiards, the coupled spin system [12] or the periodically kicked top [13].

In this work we investigate the COE–CUE transition and point out the important difference in comparison with the corresponding GOE–GUE transition. It is shown and explained why the model of the Dyson gas [14], giving a correct picture of the latter transition can not be directly applied for the circular ensembles.

In the following section, we compare the Gaussian and the circular ensembles during the OE–UE transition. We start with a somewhat formal discussion of the Dyson model and show that it provides the correct description of the transitions between different Gaussian ensembles of Hermitian matrices [15]. An analogous discussion of the circular ensembles explains why the Dyson model in its original form [14, 16] cannot describe the transition between these ensembles.

To support our observation by means of a numerical study we have chosen the model of the periodically kicked top for which special cases belonging to all three universality classes are known [6, 17]. This model is briefly recalled in section 3 where the statistical properties of the spectrum (quasi-energies) are discussed. Section 4 shows how the COE–CUE transition may be analysed by a study of the eigenvector statistics or the localization entropy. The last section contains concluding remarks and a list of open questions.

## 2. Gaussian versus circular ensembles

A transition between Gaussian ensembles of random matrices might be represented by the following model Hamilton operator [15]

$$H = H_0 + \lambda V \quad (5)$$

where  $\lambda$  is a control parameter and the operator  $V$  represented by a random matrix plays the role of a perturbation which breaks a symmetry of the system (e.g. spatial parity [3], isospin parity [18] or time-reversal symmetry [13]). The influence of the perturbation  $\lambda V$  depends on the size  $N$  of the matrix. To compare transitions for matrices of different size  $N$  it is possible to introduce a dimension-independent transition parameter  $\Lambda_D = \Lambda_D(N, \lambda)$ . For simplicity we assume  $V$  to have zero mean  $\langle V_{ij} \rangle = 0$ . The distribution of  $H$  reads

$$P_\lambda(H) = \int d[H_0] d[V] P_0(H_0) Q(V) \delta(H - (H_0 + \lambda V)) \quad (6)$$

where  $P_0(H_0)$  and  $Q(V)$  are probability distributions and  $\int d[\dots]$  denotes an integration over the ensemble. This expression can be rewritten in an obvious way as a convolution of the initial distribution of  $H_0$  with a propagator  $T_\lambda$

$$P_\lambda = P_0 * T_\lambda \quad (7)$$

$$T_\lambda(G) = \int d[V] Q(V) \delta(G - \lambda V). \quad (8)$$

Let us now remember the main idea of the Dyson model considering a Brownian motion in the space of Hermitian matrices. Time evolution of a given random matrix  $H(t)$  from time  $t$  to  $t + \delta t$  under the influence of the noise  $V$  is given by [14]

$$H(t + \delta t) = H(t) + \sqrt{\delta t} V. \quad (9)$$

This equation defines the corresponding distribution  $\tilde{P}_{t+\delta t}$  of  $H(t + \delta t)$

$$\tilde{P}_{t+\delta t} := \tilde{P}_t * T_{\sqrt{\delta t}}. \quad (10)$$

In the Dyson model the probability distribution of the noise  $Q(V)$  is given by one of the Gaussian ensembles. As a direct consequence of this particular choice of  $Q(V)$  the propagator  $T_\lambda$  has the following property:

$$T_{\lambda(t_1+t_2)} = T_{\lambda(t_1)} * T_{\lambda(t_2)}. \quad (11)$$

In the above we introduced the nonlinear rescaling between the time  $t$  and the control parameter  $\lambda$

$$\lambda(t) = \sqrt{2t}. \quad (12)$$

The Dyson model ((9) and (10)) is thus equivalent to the description given by (5), (7) and (8), because for all times  $t$  the probability distribution  $\tilde{P}_t$  is equal to  $P_\lambda$  with a given initial condition  $P_0$ . In consequence the dimension-independent transition

parameter  $\Lambda_D$  of the Dyson model is related to the control parameter  $\lambda$  of the ensemble (5) by [16, 19]

$$\Lambda_D = \lambda^2 \rho^2 \langle v^2 \rangle \quad (13)$$

where  $\rho$  represents the density of eigenvalues and  $\langle v^2 \rangle$  denotes the mean squared matrix element of  $V$ . The above relation has been verified by a numerical study of random Hermitian matrices [19].

The discussion of the circular ensembles starts with the observation that the Floquet operator of a periodically kicked system can be written in the following general form [3, 13] (see also section 3)

$$U = U_0 e^{i\kappa V} = U_0 W^\kappa \quad (14)$$

where the parameter  $\kappa$  controls the strength of the perturbation  $V$ . In analogy with (6) the distribution of the unitary matrix  $U$  may be represented by the integral

$$P_\kappa(U) = \int d[U_0] d[W] P_0(U_0) Q(W) \delta(U^{-1} U_0 W^\kappa). \quad (15)$$

This expression can also be rewritten in the form of a convolution between the initial distribution and a propagator  $T_\kappa$

$$P_\kappa = P_0 * T_\kappa \quad (16)$$

$$T_\kappa(Y) = \int d[W] Q(W) \delta(Y^{-1} W^\kappa). \quad (17)$$

The convolution over the unitary group  $f * g(Y) = \int d[W] f(W) g(W^{-1} Y)$  is a straightforward generalization of the more common definition. The delta function is normalized to unity  $\int d[W] \delta(Y^{-1} W) = 1$  and centred over unity in the sense that for all functions  $f: Y \rightarrow R$  the equation  $f(Y) = \int d[W] f(W) \delta(Y^{-1} W)$  is valid.

The Dyson model for the circular ensembles concerning a random walk in the space of the unitary matrices can be obtained in the following way:

$$U(t + \delta t) = U(t) W^{\sqrt{\delta t}}. \quad (18)$$

A motion of the distribution of  $U$  is defined by this random walk as in the case of the Gaussian ensembles. In complete analogy to (10) we get

$$\tilde{P}_{t+\delta t} = \tilde{P}_t * T_{\sqrt{\delta t}}. \quad (19)$$

The Dyson model is obtained from the process (19) by making the assumption that the matrix  $W$  is distributed according to one of the circular ensembles. In full analogy with the prediction (13) for Gaussian ensembles one obtains for the transition parameter  $K_D$

$$K_D = \kappa^2 \rho^2 \langle v^2 \rangle. \quad (20)$$

In this case  $\langle v^2 \rangle$  is the mean squared matrix element of  $V = -i \log(W)$ . A slightly different approach to the Dyson model has been proposed recently by

Pandey and Shukla [16]. They made an analogous, but equally illegitimate assumption that the random walk in the space of unitary matrices is described by  $U(t + \delta t) = U(t) \exp[i\sqrt{\delta t}V]$ , where  $V$  belongs to a Gaussian ensemble.

In contrast to the case of the Gaussian ensembles, where in (11) one used explicitly the property that a convolution of two Gaussian distributions delivers a Gaussian distribution, there is no way to reconcile (19) with the correct formulation of the transition (16), because the functional equation for  $\kappa(t)$

$$T_{\kappa(t_1+t_2)} \stackrel{!}{=} T_{\kappa(t_1)} * T_{\kappa(t_2)} \tag{21}$$

has no non-trivial solution in the circular case. The multiplication in the space of matrices is not commutative (in contrast to the addition in the space of Hermitian matrices). In consequence the convolution in the right-hand side of the above equation is not commutative, as it is imposed by the left-hand side. Therefore it has to be expected that for the time-dependent dynamical systems described by the circular ensembles the transition parameter will not be given by (20). In the following paragraphs we support this conclusion by a numerical investigation of a model system capable of showing the COE-CUE transition.

### 3. Kicked top—eigenvalues

The model of the kicked top has been known in literature for a long time. For a detailed discussion we refer to the papers of Kuś *et al* [17,20] and the work of Mikeska and Frahm [21]. The model can be considered as a spin rotating in a magnetic field and periodically twisted around perpendicular axes by nonlinear rotations. The result of one particular scenario [17] is the following Floquet operator that shifts the wavefunction from one period to the next

$$U = U_0 \exp\left[i\frac{\kappa J_x^2}{2j}\right] \quad U_0 = \exp[ipJ_z] \exp\left[i\frac{\eta J_y^2}{2j}\right]. \tag{22}$$

The parameters  $\kappa$  and  $\eta$  determine the power of the nonlinear kicks and  $p$  depends on the magnetic field. The operators  $J_i$  are the conventional angular momentum operators defined by the commutation relation  $[J_i, J_k] = i\epsilon_{ikl}J_l$ . The integer number  $j$  is the length of the spin  $J^2 = j(j + 1)$ , and is inversely proportional to Planck's constant  $\hbar$ .

For large enough values of the parameters  $p$  and  $\eta$  the eigenphases and eigenvectors of  $U_0$  have the statistical properties described by the COE [6, 17, 20, 21]. The other nonlinear kick around the  $x$ -axis destroys the generalized time-reversal symmetry [3]  $T = \exp[ipJ_z] \exp[i\pi J_x] T_0$  ( $T_0$  is the conventional time-reversal symmetry) of  $U_0$ . Therefore the operator  $U$  displays CUE fluctuations for sufficiently large values of the parameter  $\kappa$  ( $\kappa \simeq 1$ ). Making use of the fact that the quasi-energy density  $\varrho$  is proportional to  $j$  in the system studied and calculating the variance  $\langle v^2 \rangle = \langle (J_x^2/2j)^2 \rangle \propto j$ , one gets from (20) the prediction of the Dyson model for the transition parameter

$$K_D = j^3 \kappa^2. \tag{23}$$

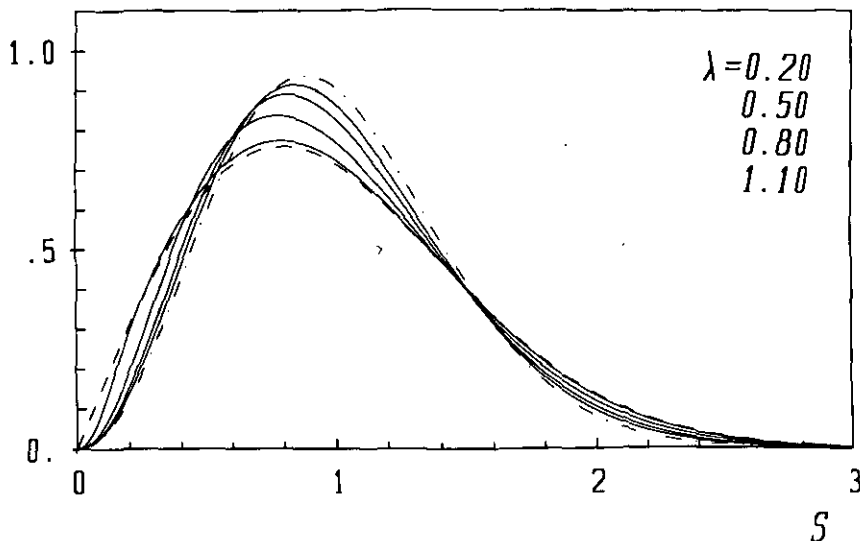
$P(S)$ 

Figure 1. The nearest-neighbour distribution (24) is plotted for several values of  $\lambda$ . The dashed curve stands for the Wigner surmise for the orthogonal ensemble and the dash-dotted curve for the unitary ensemble.

We shall now proceed to the numerical investigation of the dynamical system (22) and demonstrate differences between its transition law and the above relation resulting from the Dyson model.

The ensemble (5) describing the OE-UE transition for  $2 \times 2$  Gaussian Hermitian matrices gives a simple expression for the spacing distribution [15]

$$P(S, \lambda) = \sqrt{\frac{2 + \lambda^2}{2}} S c^2(\lambda) \exp\left[-\frac{S^2 c^2(\lambda)}{2}\right] \operatorname{erf}\left[\frac{S c(\lambda)}{\lambda}\right] \quad (24)$$

$$c(\lambda) = \sqrt{\frac{\pi(2 + \lambda^2)}{4}} \left[1 - \frac{2}{\pi} \left[\tan^{-1}\left(\frac{\lambda}{\sqrt{2}}\right) - \frac{\sqrt{2}\lambda}{(2 + \lambda^2)}\right]\right]$$

where  $\operatorname{erf}(x)$  stands for the standard error function,  $\operatorname{erf}(x) = 2/\sqrt{\pi} \int_0^x \exp[-\xi^2] d\xi$ . By varying the free parameter  $\lambda$  between 0 and  $\infty$  one gets a family of distributions interpolating between the Wigner surmises for the OE and the UE (see figure 1). Interestingly this distribution provides an approximation of the nearest-neighbour distribution of the eigenphases of the operator  $U$  defined by (22) even for large values of  $j$  to an astonishing degree of accuracy [13].

By fitting the distribution (24) to the numerically obtained nearest-neighbour distribution the following simple relation between the fitting parameter  $\lambda$  and the perturbation parameter  $\kappa$  was reported [15]:

$$\lambda = m\kappa^2. \quad (25)$$

This result, where  $m$  stands for a proportionality constant, has been confirmed by a more extensive numerical investigation. Figure 2 presents the result of fitting the

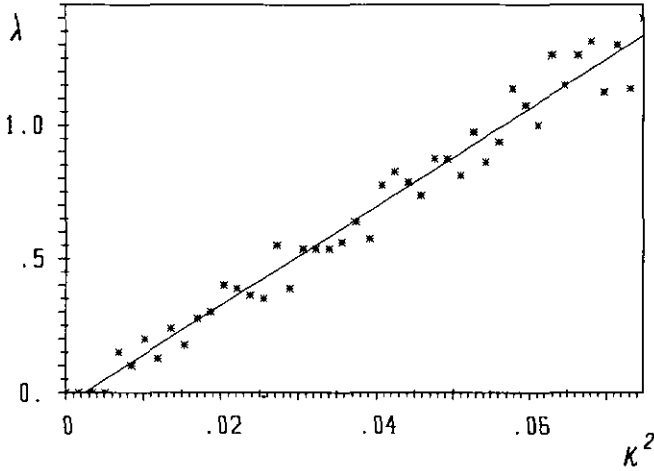


Figure 2. The control parameter  $\lambda$ , obtained by fitting equation (24) to histograms of spacing distributions of the kicked top (22), is depicted as a function of  $\kappa^2$ . The data are well approximated by a straight line.

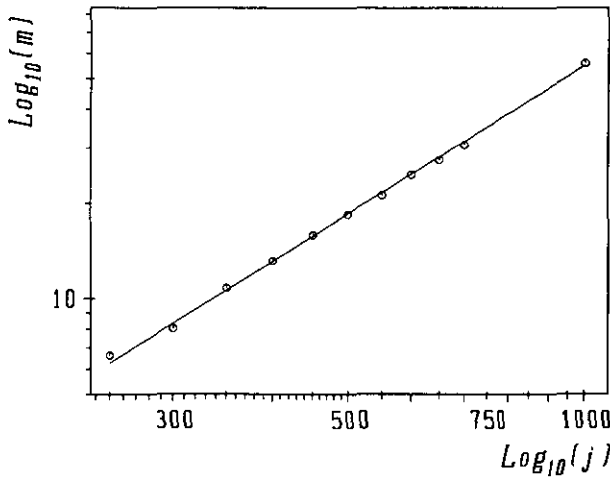


Figure 3. The logarithm of the gradient  $m$  of the straight line shown in figure 2 is plotted as function of the logarithm of  $j$ . The straight line obtained by linear regression has the slope  $\alpha = 1.53 \pm 0.04$ .

nearest-neighbour distribution of the kicked top (22) ( $j = 500$ ) with the distribution (24). Of special interest is the dependence of the coefficient  $m$  on the matrix size determined by the spin length  $j$ . By investigating matrices  $U$  of 11 different dimensions, we attained the following scaling law (see figure 3)

$$m(j) \simeq j^\alpha \tag{26}_r$$

where the best fit of the exponent  $\alpha$  gave  $\alpha = 1.53 \pm 0.04$ . Setting the value of  $\alpha$  equal to  $3/2$  and using the relation (25) one has  $\lambda \simeq j^{3/2} \kappa^2$ , where  $\lambda$  is the parameter in the distribution (24) which was obtained for a  $2 \times 2$  ensemble of Hermitian random matrices undergoing the transition (5). In the Hermitian case the

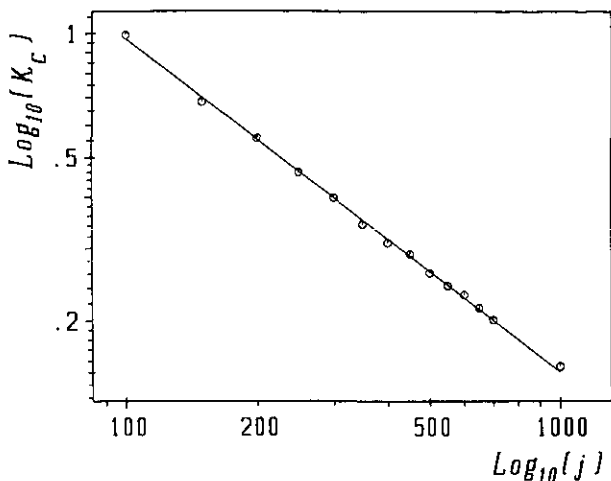


Figure 4. The logarithm of the value of  $\kappa_c$  necessary to complete the transition of the  $\Sigma^2$  statistics up to 90% is plotted as a function of the logarithm of  $j$ . By linear regression of the data points we get a straight line with gradient  $-0.81 \pm 0.03$ .

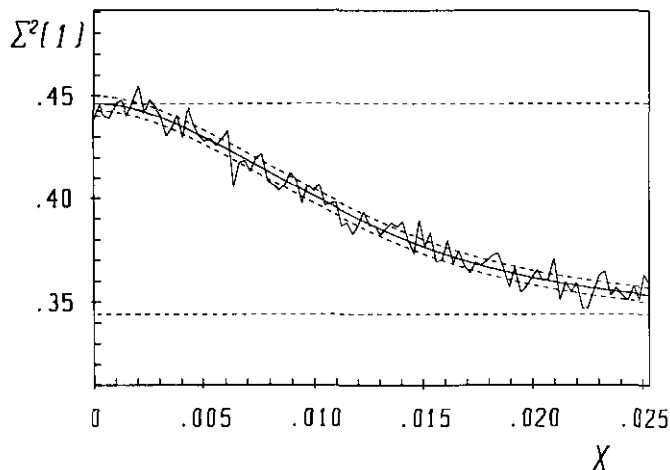


Figure 5. The numerically obtained  $\Sigma^2$  statistics ( $j = 1000$ ) is plotted as a function of  $x = \kappa^2$ . The upper dashed line is the OE value for  $\Sigma^2(1)$ , the lower dashed line the corresponding OE value. The curve is the random matrix prediction  $\Sigma^2(K)$  of [16, 22] as a function of  $x$  where  $K \simeq x^2$ . The dashed curves above and below the solid curve denote the statistical error.

dimension-independent transition parameter  $\Lambda$  given by (13) is proportional to  $\lambda^2$ . In the same manner we treat the unitary ensembles and define a dimension-independent transition parameter  $K_e \simeq \lambda^2$ . The experimentally found dependence reads

$$K_e = j^3 \kappa^4 \quad (27)$$

in a clear discrepancy with the prediction (23) of the Dyson model. Since the distribution (24) was found for Hermitian  $2 \times 2$  matrices this argument is not rigorous and has to be confirmed in an independent way by studying a measure for which precise



predictions of the random matrix theory are known. For this purpose we shall use the number variance [1, 22]. This quantity calculated for unfolded spectra with an average nearest neighbour spacing of unity ( $\langle S \rangle = 1$ ) is equal to the variance of the number of eigenvalues  $n$  in a stretch of length  $L = \langle n \rangle$  of the quasi-energy axis

$$\Sigma_{(j,\kappa)}^2(L) = \langle (n - \langle n \rangle)^2 \rangle \quad (n) = L. \tag{28}$$

To study the scaling behavior of the transition we evaluated a critical value of  $\kappa_c$ , necessary to complete the transition OE-UE (for  $L = 1$ ) up to 90%

$$\Sigma_{(j,\kappa_c)}^2(1) = \Sigma_{\text{UE}}^2(1) + 0.1(\Sigma_{\text{OE}}^2(1) - \Sigma_{\text{UE}}^2(1)). \tag{29}$$

The result of the numerical calculation is shown in figure 4. In agreement with our former result we obtain

$$\kappa_c \simeq j^{-\alpha/2} \tag{30}$$

where in this case the numerically obtained value of the exponent is  $\alpha = 1.62 \pm 0.06$ . The transition curve obtained numerically with  $j = 1000$  for  $\Sigma^2(1)$  as a function of  $\kappa^2$  is depicted in figure 5. The solid denotes the theoretical prediction obtained by Mehta and Pandey [22] for  $\Sigma^2(K_D)$ . If we replace the relation (20) ( $K_D \simeq \kappa^2$ ) by a more general trial statement  $K_D \propto \kappa^\nu$  we get a perfect coincidence between the data and the theoretical curve for  $\nu = 4.0 \pm 0.2$ . This procedure has been repeated for several values of  $j$  and  $L$ , providing a convincing argument that

$$K_e = j^3 \kappa^4 \tag{31}$$

is the appropriate parameter for the COE-CUE transition.

#### 4. Kicked top—eigenvectors

Eigenvector statistics provides, beside the eigenvalue statistics, a sensitive indicator for chaos in the underlying classical system [6, 23, 24]. Therefore we also investigated the scaling behaviour of the eigenvector statistics for the transition COE-CUE. We already reported [23] that it is possible to describe the distribution of the modulus of an eigenvector component  $y = |\langle n | \phi \rangle|^2$  between the orthogonal and unitary case by a simple expression

$$P_b(y) = \frac{b}{2\sqrt{b-1}} \exp\left[-\frac{yb^2}{4(b-1)}\right] I_0\left(\frac{(2-b)by}{(b-1)4}\right) \quad b \in [1, 2] \tag{32}$$

where  $I_0$  denotes the modified Bessel function. When  $b$  changes between 1 and 2 the distribution (32) is transformed from the  $\chi_\beta^2$  distribution (4) with  $\beta = 1$  (OE) to the  $\chi_\beta^2$  distribution (4) for  $\beta = 2$  (UE). To study the scaling behaviour of the eigenvectors we evaluated the critical value of the kick strength  $\kappa^c$  necessary to obtain a prescribed value of the fitting parameter  $b$

$$P_{(j,\kappa^c)}(y) = P_b(y). \tag{33}$$

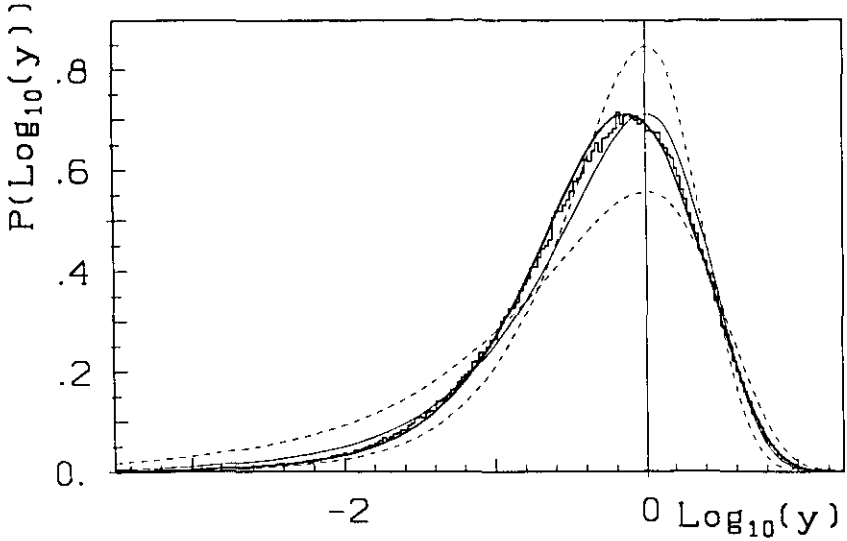


Figure 6. Eigenvector statistics of the top (21) with  $j=200$ ,  $\kappa = 0.27$ . The thick solid curve denotes the best fit of  $P_b(y)$ , ( $b = 1.18$ ), the thin solid curve the best fit of  $P_\beta(y)$ , ( $\beta = 1.5$ ). The dashed curves correspond to  $P_{\beta=1}(y)$ , (OE) and  $P_{\beta=2}(y)$  (UE).

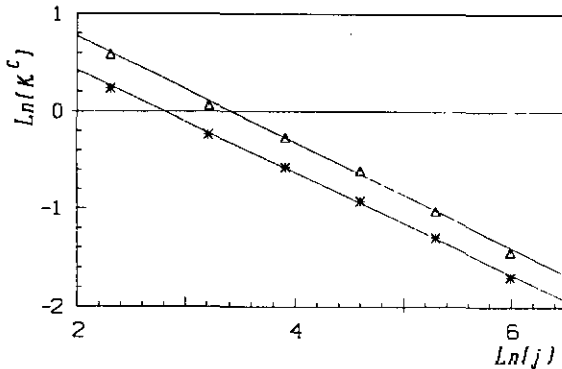


Figure 7. Dependence of the critical values of  $\kappa^c$  on the dimension  $j$  on a logarithmic scale. The fitted straight lines confirm the scaling behaviour of the eigenvector statistics. The slopes of the straight lines are:  $-0.52$  (for the lower curve,  $b = 1.18$ ) and  $-0.54$  (for the upper curve,  $b = 1.42$ ).

The distribution  $P_{(j, \kappa^c)}(y)$  denotes the experimental result obtained for given values of  $j$  and  $\kappa^c$  (note that the value of the critical strength  $\kappa^c$  might be different from that entering (29) and (30)). Figure 6 shows a result of such an evaluation of  $\kappa^c$  for  $b = 1.18$ . This procedure has been repeated for a number of dimensions  $j$  and another value of  $b = 1.42$ . The result is presented in figure 7. It follows that the transition parameter for eigenvectors  $\tilde{K}_e$  is

$$\tilde{K}_e = j\kappa^2. \tag{34}$$

The Dyson model predicts the same scaling law ( $K_D = j^3\kappa^2$ ) for the transition measures concerning eigenvalues and eigenvectors [19, 25]. In our study we have

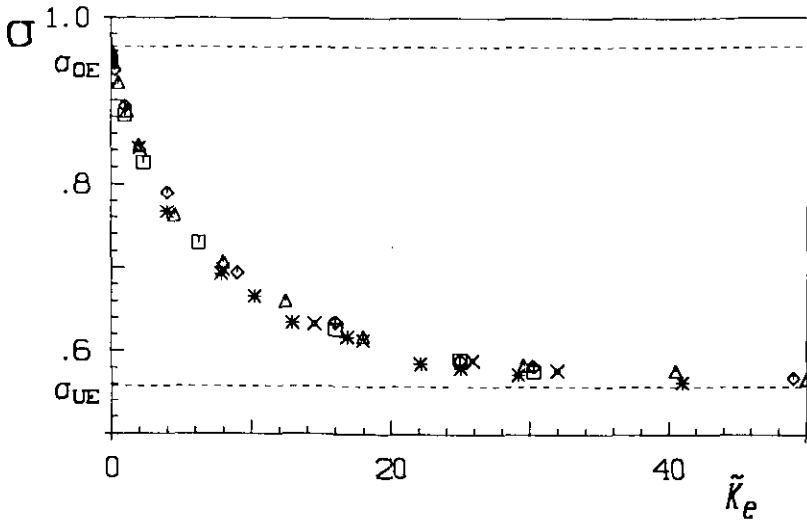


Figure 8. Width of the eigenvector distribution  $\sigma$  as a function of the transition parameter  $\tilde{K}_e = j\kappa^2$  for  $j = 400$  stars,  $j = 200$  crosses,  $j = 100$  diamonds,  $j = 50$  triangles,  $j = 25$  squares. The dashed horizontal lines denote the limiting values for OE and UE.

shown that the statistical properties of eigenvectors have a different scaling law. The transition rate for the eigenvectors is slower in the sense that the dimension-independent transition parameter is proportional to  $j^{3/2}$  for eigenvalues and to  $j$  for the eigenvectors. This is in agreement with a random matrix model designed to mimic the transition between regular and chaotic motion [26]. To study the transition of the eigenvector distribution in another independent way, we looked at the variance of the variable  $\log_{10}[y]$

$$\sigma^2 = \int_0^\infty dy P(y) (\log_{10}(y) - \langle \log_{10}(y) \rangle)^2. \tag{35}$$

For the three universality classes  $\beta = 1, 2, 4$  one attains

$$\sigma^2(\beta) = \frac{\zeta(2, \beta/2)}{\ln(10)^2} \tag{36}$$

where  $\zeta$  is the zeta function of Riemann [27]. For the interesting limiting cases of the orthogonal and the unitary ensemble one has

$$\sigma_{OE} = \frac{\pi}{\sqrt{2} \ln(10)} \sim 0.96 \quad \sigma_{UE} = \frac{\pi}{\sqrt{6} \ln(10)} \sim 0.56. \tag{37}$$

During the transition  $\sigma$  decreases monotonously starting from  $\sigma_{OE}$  to  $\sigma_{UE}$ . This quantity may therefore be used as an indicator for time-reversal symmetry breaking, in a similar manner as  $\Sigma^2(L)$ . Unfortunately no relation between the parameters  $b$  and  $\kappa$  is known. To check the scaling law (34) we plotted in figure 8 the mean square deviation  $\sigma$  as a function of the transition variable  $\tilde{K}_e = j\kappa^2$  for various values of  $j$  and  $\kappa$ . It is evident that all points lie at one single curve. We have therefore confirmed the scaling law (34) in a complementary way.

It is worth stressing that the statistical properties of eigenvectors may also be studied by other quantities such as the Shannon entropy, the localization length or the inverse participation ratio. All these statistical measures vary with the same rate as the variance  $\sigma$  or the critical kick strength  $\kappa^c$  in contrast to the statistical measures of the spectral fluctuations like  $\Sigma^2$ .

## 5. Concluding remarks

Transitions between different universality classes of Gaussian ensembles are well described by the Dyson model of Brownian motion in space of random Hermitian matrices. This approach is useful to represent the process of breaking of the time-reversal symmetry in classically chaotic, conservative systems, which corresponds to the GOE–GUE transition.

The classically chaotic, time-dependent periodically driven systems are described by the circular ensembles of unitary matrices. Our study shows that the original Dyson model of random walk is not capable of characterizing the analogous transitions between circular ensembles. Numerical analysis of a simple dynamical system—a periodically driven top—revealed a different scaling of the transition COE–CUE than that predicted by the Dyson model and reported for the Gaussian ensembles. Moreover, it has been shown that the transition rate is different when concerning the properties of the spectrum (eigenvalues) and the Shannon entropy or localization length (eigenvectors).

The original version of the Dyson model fails to correctly describe transitions between circular ensembles. However a fair coincidence with the numerical data is regained when ansatz (31) is made. It is not at all clear why such an assumption provides a correct prediction of the transition rate. This point might be clarified by a rigorous investigation of the ensemble defined by equation (16), which is obviously not equivalent to the ensemble of unitary matrices determined by the Dyson process.

Further work is needed to find a necessary modification of the Dyson model in order to make it applicable for circular ensembles. The numerical investigation of the modified model should be performed not only on the dynamical systems like the kicked top but also directly on the random unitary matrices—members of the circular ensembles.

## Acknowledgments

We have enjoyed fruitful discussions with F Haake, M Kuś and M R Zirnbauer. Financial support by the Sonderforschungsbereich ‘Große Unordnung und Fluktuationen’ SFB 236 of the deutschen Forschungsgemeinschaft and by the project nr 2-007901 of Polski Komitet Badań Naukowych is gratefully acknowledged. One of us (GL) was also supported by the DFG-PAN project ‘Kwantowe aspekty dynamiki nieliniowej’.

## References

- [1] Mehta M L 1990 *Random Matrices* (New York: Academic)

- [2] Bohigas O 1989 *Chaos and Quantum Physics (Les-Houches Session LII)* ed M J Giannoni and A Voros (Amsterdam: North-Holland)
- [3] Haake F 1991 *Quantum Signatures of Chaos* (Berlin: Springer)
- [4] Scharf R, Dietz B, Kuś M, Haake F and Berry M V 1988 *Europhys. Lett.* **5** 383
- [5] Brody T A, Flores J, French J B, Mello P A, Pandey A and Wong S S M 1981 *Rev. Mod. Phys.* **53** 385
- [6] Kuś M, Mostowski J and Haake F 1988 *J. Phys. A: Math. Gen.* **21** L1073
- [7] Berry M V and Tabor M 1977 *Proc. R. Soc. A* **356** 375
- [8] Porter C E 1965 *Statistical Theories of Spectra* (New York: Academic)
- [9] Imry Y 1986 *Europhys. Lett.* **1** 249
- [10] Mailly D, Sanquer M, Pichard J L and Piri P 1989 *Europhys. Lett.* **8** 471
- [11] Berry M V and Robnik M 1986 *J. Phys. A: Math. Gen.* **19** 649
- [12] Puri R and Haake F 1992 to be published
- [13] Lenz G and Haake F 1991 *Phys. Rev. Lett.* **67** 1
- [14] Dyson F J 1962 *J. Math. Phys.* **3** 1191
- [15] Lenz G and Haake F 1990 *Phys. Rev. Lett.* **65** 2325
- [16] Pandey A and Shukla P 1991 *J. Phys. A: Math. Gen.* **24** 3907  
Pandey A and Shukla P 1991 Circular ensembles and quantum chaos: a semiclassical theory of spectral correlation *Preprint*
- [17] Kuś M, Scharf R and Haake F 1987 *Z. Phys. B* **66** 129
- [18] Guhr T and Weidenmüller H A 1990 *Ann. Phys., NY* **199** 412
- [19] French J B, Kota V K B, Pandey A and Tomsovic S 1988 *Ann. Phys., NY* **181** 198, 235
- [20] Haake F, Kuś M and Scharf 1987 *Z. Phys. B* **65** 381
- [21] Frahm H and Mikeska H J 1988 *Phys. Rev. Lett.* **60** 3
- [22] Pandey A and Mehta M L 1983 *Commun. Math. Phys.* **87** 449
- [23] Życzkowski K and Lenz G 1991 *Z. Phys. B* **82** 299
- [24] Haake F and Życzkowski K 1990 *Phys. Rev. A* **42** 1013
- [25] Tanaka S and Sugano S 1986 *Phys. Rev. B* **34** 6880
- [26] Lenz G, Życzkowski and Saher D 1991 *Phys. Rev. A* **44** 8043
- [27] Abramowitz M and Stegun I A 1984 *Pocketbook of Mathematical Functions* (Frankfurt-am-Main: Harri Deutsch)